Tailoring phase-space in neutron beam extraction

S. Weichselbaumer[a], G. Brandl[a,b], R. Georgii[a,b], J. Stahn[c], T. Panzner[d], P. Böni[b]

[a]*Heinz Maier-Leibnitz Zentrum und Physik-Department E21, Technische Universität München, Lichtenbergstr. 1, D-85748 Garching, Germany*
[b]*Physik-Department E21, Technische Universität München, James-Franck-Str. 1, D-85748 Garching, Germany*
[c]*Laboratory for Neutron Scattering, Paul Scherrer Institut, CH-5232 Villigen PSI, Switzerland*
[d]*Material Science and Simulations, Neutrons and Muons, Paul Scherrer Institut, CH-5232 Villigen PSI, Switzerland*

arXiv:1406.1313v2 [physics.ins-det] 3 Mar 2015

Abstract

In view of the trend towards smaller samples and experiments under extreme conditions it is important to deliver small and homogeneous neutron beams to the sample area. For this purpose, elliptic and/or Montel mirrors are ideally suited as the phase space of the neutrons can be defined far away from the sample. Therefore, only the useful neutrons will arrive at the sample position leading to a very low background. We demonstrate the ease of designing neutron transport systems using simple numeric tools, which are verified using Monte-Carlo simulations that allow to take into account effects of gravity and finite beam size. It is shown that a significant part of the brilliance can be transferred from the moderator to the sample. Our results may have a serious impact on the design of instruments at spallation sources such as the European Spallation Source (ESS) in Lund, Sweden.

Keywords: Neutron scattering, European Spallation Source, Neutron guides, Elliptic guides, Montel mirrors, Supermirror, Monte-Carlo simulations, McStas

1. Introduction

The foundation laying for the European Spallation Source (ESS) in Lund, Sweden took place in October 2014. ESS is intended to operate at a power of 5 MW and will use a long-pulse target station for the neutron production. The resulting, time-integrated flux will be comparable or even larger than the continuous flux at the high flux reactor HFR at the Institut Laue-Langevin in Grenoble [1]. However, the peak flux at ESS will exceed the time-averaged flux of the ILL by at least a factor of 30. Therefore, using time-of-flight techniques the performance will be largely increased. Further increases will be possible by implementing modern neutron transport systems based on non-linearly tapered neutron guides and a clever design of the instruments.

For more than three decades, with the invention of neutron guides by Maier-Leibnitz [2], neutrons were transported over large distances mostly by Ni-coated, straight or curved guide tubes. However, due to the small critical angle of total reflection given by $\theta\,/\,^\circ = 0.099 m\lambda\,/\,\text{Å}$, where $m = 1$ for Ni, the transport was only efficient for cold neutrons. Using supermirror coatings, the index m was increased up to $m = 7$ [3] thus allowing to even transport epithermal neutrons with wavelength of 1Å at spallation sources.

Due to the many internal reflections of the neutrons in straight high-m neutron guides, however, the transmission is seriously reduced [4]. Moreover, the significant losses require massive shielding of the neutron guides. Mezei [5] and Schanzer et al. [6] proposed the use of a truly bent elliptic neutron guides, which reduce the number of reflections to essentially two. These guides are focusing the neutrons from the moderator exit to the sample in terms of the point to point imaging provided by an ellipse in mathematics [7]. For example, the replacement of the straight neutron guide at the beam line HRPD at ISIS by a 90 m long elliptic guide increased the neutron flux at the sample by up to two orders of magnitude [8]. In addition, as the beam paths can be simply identified using geometrical optics, it is straightforward to design and judge the performance of elliptic guides [9]. Recently Klenø et al. have shown that approximately 50% to 90% of the brilliance of cold (4.25 Å $\leq \lambda \leq$ 5.75 Å) and thermal (0.75 Å$\leq \lambda \leq$ 2.25 Å) neutrons can be transported from the moderator to the sample using parabolic or elliptic guide geometries [10]. Effects of gravity were included in this study.

Often, it is argued that elliptic guides are prone to a large background at the sample because there is a direct view to the moderator. However, by inserting beam blockers in the central part of the guide, the line of sight can be effectively interrupted [11] without affecting the homogeneity of the beam. It is correct, that the blocker leads to a hole in the transmitted phase space as pointed out by Zendler et al. [12]. However, this hole is very small, as for instance in our simulation of the order of 0.12° (see Fig.7b) and is therefore swamped by effects of waviness if real neutron guide systems are considered [9]. The major background of elliptic guides is caused by the fast neutrons that emerge from the neutron source and illuminate the internal surfaces of the guide close to the sample [9]. These neutrons can effectively be stopped by placing two or more elliptic guides in series [11] with the further advantage that effects of halo and coma aberration are reduced, if an even number of guides is used. Then even beam blockers may become superfluous. The direct line of sight can also be interrupted by gravitational curv-

Email address: Robert.Georgii@frm2.tum.de (R. Georgii)

ing of long neutron guides [13].

Amongst the other guide concepts, Montel guides are very promising in delivering neutrons to the sample. These mirrors were invented by Montel in 1957 for focusing X-rays [14] and have now become an integral part of many beam lines at synchrotron sources and for x-ray diffractometers. Recently, Montel mirrors have been used by G. Ice for the focusing of neutron beams [15]. Stahn et al. use them for reflectometry, i.e. for the SELENE project [16]. In addition, a guide system based on Montel mirrors was optimized for a proposed MIEZE type spin echo spectrometer for the ESS [17].

A Montel mirror consists of two elliptic mirrors that are arranged perpendicular to each other, i.e. the optics consists of a "quarter" of a four-sided elliptic neutron guide. In the center of the Montel mirror a beamstop can be placed for defining the accepted divergence independent from the beam size which is defined by the entrance aperture. Because the Montel mirror is inclined in the horizontal and vertical direction the direct line of sight is interrupted leading to an excellent signal-to-noise ratio on the sample.

Montel mirrors have many advantages when compared with other concepts for neutron guides. Beside of the advantage of tailoring the neutron beam more than typically ten meters away from the sample position [18], the path of the neutrons through the optical system is clear, i.e. it takes place via two reflections in each device. Moreover, the brilliance transfer can easily be evaluated based on reflectivity data of the supermirrors.

The aim of the present work is, firstly, to evaluate the performance of various types of neutron guides, including elliptic, Montel and straight guide systems, using geometrical optics and analytical tools (Fig. 1). In a second step we will verify the numeric results using the Monte-Carlo simulation package McStas [19]. The results show that it is indeed possible to calculate the performance for small beam and sample sizes and ignoring gravity rather accurately using simple analytical means. Finally, gravitational effects will be taken into account using Monte-Carlo simulations.

2. Numeric calculations without gravity

In a first step we calculate the angle of reflection of neutrons emerging from a point source at the first focal point A of the ellipse, hitting the mirror at the point P and arriving at the second focal point B (Fig. 2). If the contour of the ellipse is represented by a parametric equation in polar coordinates, the distance r is given by

$$\overline{AP} = r(\theta) = \frac{a(1-e^2)}{1-e\cos\theta} \tag{1}$$

where $e = L/2a$ is the numerical eccentricity of the ellipse, $L = 2\sqrt{a^2-b^2}$ is the distance between the focal points A and B, and a and b are the half axes of the ellipse. The local angle of reflection, γ, is given by

$$\gamma = \frac{\pi}{2} - \frac{\alpha+\beta}{2}, \tag{2}$$

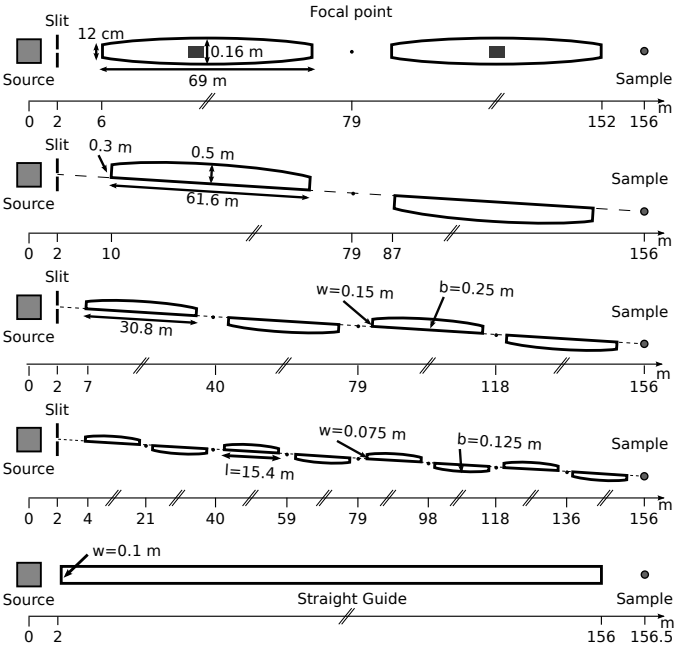

Figure 1: The different extraction methods and guide designs in this paper are shown in a top view for comparison. In order from top to bottom these are a double elliptic guide, the 2-fold and the 4-fold Montel guides and a classical straight guide to get out of the direct sight of the moderator. All mirrors have a $m = 7$ coating. The beam stop in the elliptic guide has a height of 0.14 m and is absorbing all neutrons, which have not been reflected. The Montel guides are inclined by 1.25° in both horizontal and vertical direction (not drawn here).

where

$$\alpha = \frac{\pi}{2} - \theta, \quad \beta = \arccos\left(\frac{r\,\sin\theta}{2a-r}\right). \tag{3}$$

γ can then be used to calculate the reflectivity $R'(\lambda,\gamma)$ of the supermirror in dependence of the neutron wavelength λ and eventually the transmitted intensity can be determined for all wavelengths.

In the following, a point-like source and a $m = 7$ supermirror (which is currently state-of-the-art) is assumed for all guides. The reflectivity profile of the supermirror is parametrized by assuming a constant reflectivity $R = 1$ up to a critical value $Q_c = 0.0219\,\text{Å}^{-1}$ (corresponding to $m = 1$) followed by a linear decrease to $R = 0.5$ at $q = m \cdot Q_c = 7Q_c$. The transmitted

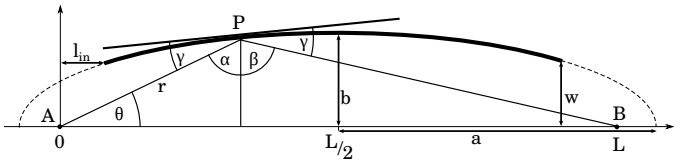

Figure 2: Schematic view of an elliptic mirror. a and b are the semi-major and semi-minor axis, respectively. L is the distance between the focal points A and B. The angles α and β can be used to calculate the reflection angle γ of the neutron trajectory with the surface of the ellipse at the point P. w and l_{in} are the distance of the guide to the central axis and the distance between the focal point to the guide entry, respectively.

neutron intensity for a specific wavelength can be determined by integrating the reflectivity along the whole mirror:

$$R(\lambda) = \frac{1}{\theta_1 - \theta_0} \int_{\theta_0}^{\theta_1} R'(\lambda, \theta)\, \mathrm{d}\theta, \tag{4}$$

where $\theta_0 = \arctan(w/(L - l_{\mathrm{in}}))$ and $\theta_1 = \arctan(w/l_{\mathrm{in}})$ (see fig. 2) are the angles which define the accepted divergence. w and l_{in} are the distance of the guide to the central axis and the distance between the focal point to the guide entry, respectively. To obtain the intensity for n Montel mirrors, the reflectivity has to be taken to the power of $2n$ since a neutron is reflected twice by each Montel mirror.

The numeric results are valid in the limit of beams with no divergence. Therefore we verified them by using Monte Carlo simulations choosing for the in and outgoing beam a size $5 \times 5\,\mathrm{mm}^2$ with a small divergence of $\pm 0.25^o$. To compare the different guide concepts we use the brilliance transfer (BT) as it was defined by Klenø et al. [10]. The brilliance or phase space density Ψ is the number of neutrons per unit time, area, solid angle and wavelength interval. According to Liouville's theorem the brilliance transfer $\mathrm{BT} = \Psi_{\mathrm{entry}}/\Psi_{\mathrm{sample}}$ can never be larger than one. To measure the BT we place monitors with the same restriction in size, wavelength and divergence after the entry slit (for the straight guide in front of the guide entry) and at the sample position.

Fig. 3 shows that the Monte Carlo simulations match the functional form of the numeric predictions very nicely and predict in the case of the Montel optics even correctly the BT. The smaller then predicted BT for the elliptic guides can be attributed to the absorption of neutrons in the beam stop in the elliptic guides which is not included in the analytical model. Due to the small divergence used this effect is particularly strong in Fig. 3 and will be less prominent in the simulations with larger divergence of $\pm 1^o$ which will be used in the following section.

In the light of these results, whenever possible, numeric calculations for the design of neutron guides should be conducted first to provide independent tests of the correct placement of the guides in the simulations. It allows also for first estimations of the efficiency of a neutron guide system facilitating and speeding up the comparison of different designs. However, to include the effects of larger beam and sample sizes and the effect of gravity Monte-Carlo simulations are required.

3. Inclusion of effects of gravity

In the following we investigate the effect of gravity on the performance of the transport systems discussed above. Gravitational effects are large: For example, neutrons with $\lambda = 5$ Å drop 193 mm along a free flight path of 156 m. Due to the complexity of the problem, Monte-Carlo simulations are mandatory.

For all simulations in this section a flat wavelength spectrum with a brilliance of $\Psi = 1 \times 10^{12} \mathrm{cm}^{-2}\mathrm{s}^{-1}\mathrm{Å}^{-1}\ \mathrm{sterad}^{-1}$ for $1\,\mathrm{Å} \le \lambda \le 15\,\mathrm{Å}$ is considered. The divergence at the sample is assumed to be $\pm 1^\circ$. An aperture with an opening corresponding to the assumed sample size is placed at the position of the closest place for a neutron guide at the ESS, i. e. 2 meters away from the moderator (see Fig. 1). For the straight guide a cross section of $100 \times 100\,\mathrm{mm}^2$ and no entry slit is assumed. A quantitative comparison of the normalized intensity transported through the guide system and the brilliance transfer (BT) for the different neutron guide systems is shown in Fig. 4 for an aperture of $5 \times 5\,\mathrm{mm}^2$. The difference here is, that the upper plot shows the intensity normalized to the guide entry whereas the BT shows the brilliance at the sample position normalized to the brilliance at the entry slit. In Tab. 1 the effect of gravity is given for the different guide systems as the ratio of the integrated intensities without and with gravity. Furthermore the signal–to–noise ratio (SNR), defined as ratio of the integrated intensity on a sample of size of $5 \times 5\,\mathrm{mm}^2$ to the total transported integrated intensity is given.

The major disadvantages of a straight guide are the reflection losses, which increase the shielding effort considerably and the illumination of the surroundings close to the sample thus increasing the background and reducing the signal-to-noise ratio (c.f. Fig. 7 a and Tab. 1). On the contrary gravity has no effect on the performance of straight guides (the ratio in Tab. 1 is equal to 1) as it only leads to slightly larger angles of reflection

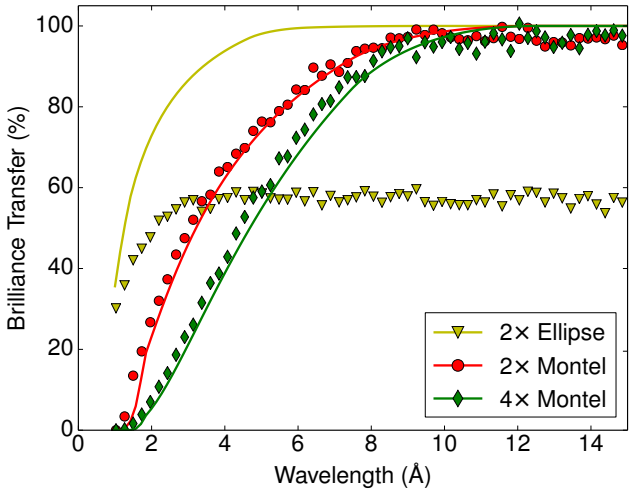

Figure 3: Comparison of the BT of the double elliptic guide system and the 2-fold and 4-fold Montel mirror systems (all $m = 7$) versus wavelength. The solid lines are the analytically calculated curves and the data points are the result of Monte-Carlo simulations. The simulations where performed without taking effects of gravity into account. The opening of the entry slit and the sample size is $5 \times 5\,\mathrm{mm}^2$ and the divergence $\pm 0.25^o$.

Config.	**No gravity** I_{NG} (s^{-1})	**Gravity** I_{G} (s^{-1})	**Ratio** $I_{\mathrm{NG}}/I_{\mathrm{G}}$	**SNR** (%)
2 x Ell.	5.7×10^8	3.4×10^8	1.7	57
2 x Mon.	$6. \times 10^8$	4.6×10^8	1.3	90
4 x Mon.	3.3×10^8	2.9×10^8	1.1	91
Straight	4.6×10^8	4.6×10^8	1.0	0.25

Table 1: Integrated intensities on a $5 \times 5\,\mathrm{mm}^2$ sample for a wavelength band of 2 Å – 6 Å for the different configurations. A ratio close to 1 means that gravity has only a small effect on the transport properties. The SNR (Signal-to-Noise ratio) specifies how much intensity arrives in the case for enabled gravity inside the sample rectangle shown in Fig. 7a compared to the overall intensity on the position sensitive detector (PSD).

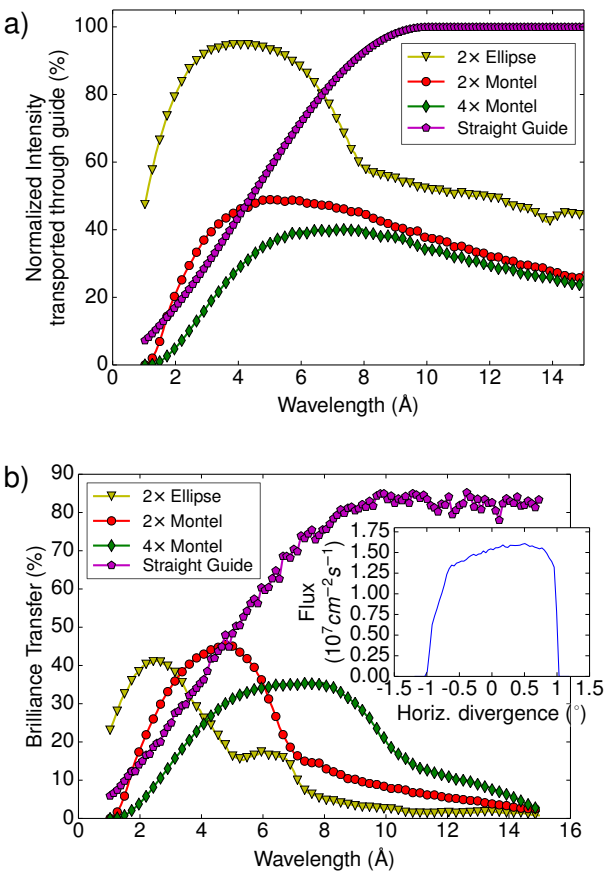

Figure 4: (a) The integrated intensity after the guide exit vs. wavelength normalized to the intensity at the guide entry and (b) the brilliance transfer vs. wavelength for different guide geometries respecting the effects of gravity. The inset shows the divergence distribution at the sample position. The BT for the Montel optics peaks at different λ depending on the number of mirrors. The beam size and sample size was $5 \times 5\,\mathrm{mm}^2$. The inset shows the horizontal divergence of the 2-fold Montel system at the sample position.

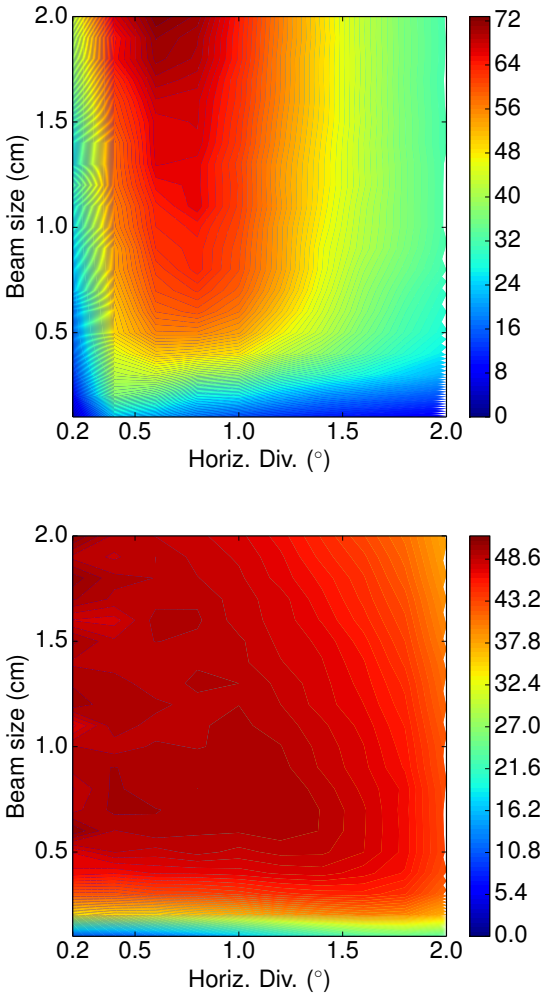

Figure 5: The BT in dependence of beam size and beam divergence for (a) the dual ellipse and (b) a 2-fold Montel guide for a wavelength of 4Å. The ellipse is better for larger sample sizes whereas the Montel mirrors are better suited for smaller sample sizes.

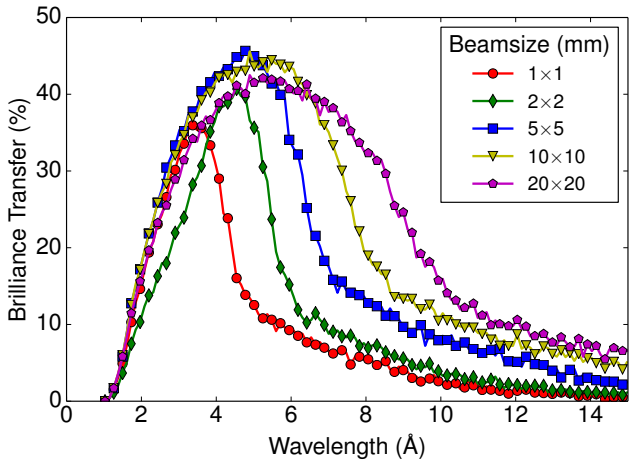

Figure 6: Comparison of the BT of a 2-fold Montel system for various beam sizes. Effects of gravity are taken into account. The aperture at the entry and the detector at the sample position have the same size as given in the legend.

for neutrons when they are "hopping" along the guide. As it is relative easy and cheap to produce and transports large beams over a large wavelength band without big losses it is widely used in neutron facilities.

The elliptic guide transports nearly all neutrons in a wavelength range of 2 Å – 6 Å (see figure 5) with a BT up to 72%, mainly for larger beam sizes. A detailed analysis of the BT for elliptic guides has been performed by Klenø et al. [10]. They obtain a similar larger BT for a λ = 1.5 Å and a m=3 guide. As seen from the spatial distribution in Fig. 7a the relatively low SNR of 57% (see Tab. 1) is due to half of the neutrons missing the sample. Furthermore this type of guides is sensitive to gravity, the beam decreases in size and in intensity and the integrated intensity on the sample decreases by a factor of 1.7. The elliptic guide is well suited for shorter wavelength for reducing the background at the sample compared to the straight guide.

With enabled gravity the 2-fold and the 4-fold Montel systems provide the best performance in the wavelength range of 2 Å – 6 Å. They deliver only neutrons which hit the sample giving a very high SNR of 90 % (see Fig. 7a and Tab. 1). For guides composed of Montel mirrors the sensitivity to gravity is less as for elliptic guides. As the maximum of the BT shifts with increasing number of mirrors to longer wavelengths for each application the appropriate system needs to be chosen. The 2-fold Montel is ideal for delivering neutrons with an excellent signal-to-noise ratio to small samples in a wavelength range between 3 Å – 6 Å.

Fig. 6 shows the performance of the 2-fold Montel system versus sample size with gravity enabled. The width of the wavelength band $\Delta\lambda/\lambda$ with high BT increases from $\simeq$ 0.56 to $\simeq$ 1.2 when the sample size is increased from 1 mm × 1 mm to 20 mm × 20 mm. The optimum BT is obtained for samples $5 \times 5\,\mathrm{mm}^2$ and 3 Å $\leq \lambda \leq$ 6 Å, a parameter range that will be discussed in more detail in the following, as it will be of great interest for many instrument designs for the ESS [20].

In Fig. 7 the spatial and divergence distribution on the sample is given for a 2-fold Montel mirror with an entry aperture size of $5 \times 5\,\mathrm{mm}^2$. The assumed sample size of $5 \times 5\,\mathrm{mm}^2$ is indicated in part a) of this figure by white rectangles and the maximal intensity is normalized for better comparison. Neutrons may not hit the sample i) due to reflection losses or ii) due to arriving outside the white rectangles thus contributing to the background.

The top row of the image shows the spatial and divergence distribution for the dual ellipse system. A considerable part of the neutrons arrive outside the sample. Also note the gap in the divergence distribution which is caused by the beam blocker. In rows two and three one can clearly see the effects of an increasing number of mirrors. For increasing number of Montel mirrors the homogeneity of the spatial and divergence distribution increases. The four mirror systems leads to a very homogeneous illumination of the sample area both for spatial and divergence coordinates. The straight guide system shows a very homogenous spatial and divergence distribution, although the majority of neutrons does not contribute to the sample illumination.

4. Conclusions

We have shown that multiple elliptic guides and Montel mirror systems provide an efficient neutron transport from the moderator to the sample. As the selection of the phase space is conducted close to the moderator, the background outside the biological shielding of the neutron source is massively reduced leading to a very low background at the sample position. As a side-effect, the costs for shielding are reduced. Using geometrical optics the brilliance transfer (BT) can be easily calculated if beam size and gravitational effects are neglected, which is possible for short guide systems. Monte-Carlo simulations show that for the assumed unfavorable conditions we considered, i.e. long flight paths of 156 m and small sample size lead to BTs of 40%. Almost all of the neutrons transported through the guide system reach the sample and there will be practically no background. To quantify this we consider for an example the thermal beam port H12 at the ILL with its brilliance at λ = 4 Å of $\Psi = 4 \times 10^{12}\mathrm{cm}^{-2}\mathrm{s}^{-1}\text{Å}^{-1}$ sterad^{-1} [1]. Using

$$I = \Psi \times A \times \Omega \times \Delta\lambda \times BT \tag{5}$$

and assuming a $\Delta\lambda/\lambda$ = 2 Å and a horizontal and vertical divergence of $\pm 1^o$, we end up with 2×10^9 neutrons per second hitting on the sample with an area A = 5 mm^2. For the ESS similar time averaged intensities with no background can be expected.

For high throughput of large beams and low background, a double elliptic guide system using small entrance and exit to reduce the number of reflections $N > 2$ (i.e. focusing configuration) may be the optimum choice. Finally, when choosing the optimum guide geometry the perfection of the mirrors should be respected. Presently, Montel mirrors and neutron guides have a waviness of $\simeq 1.0 \cdot 10^{-5}$ rad and $\simeq 1.0 \cdot 10^{-4}$ rad, respectively, leading to a blurring of the beam over a distance of 100 m of 1 mm and 10 mm, respectively. These values should be compared with the effects of gravity.

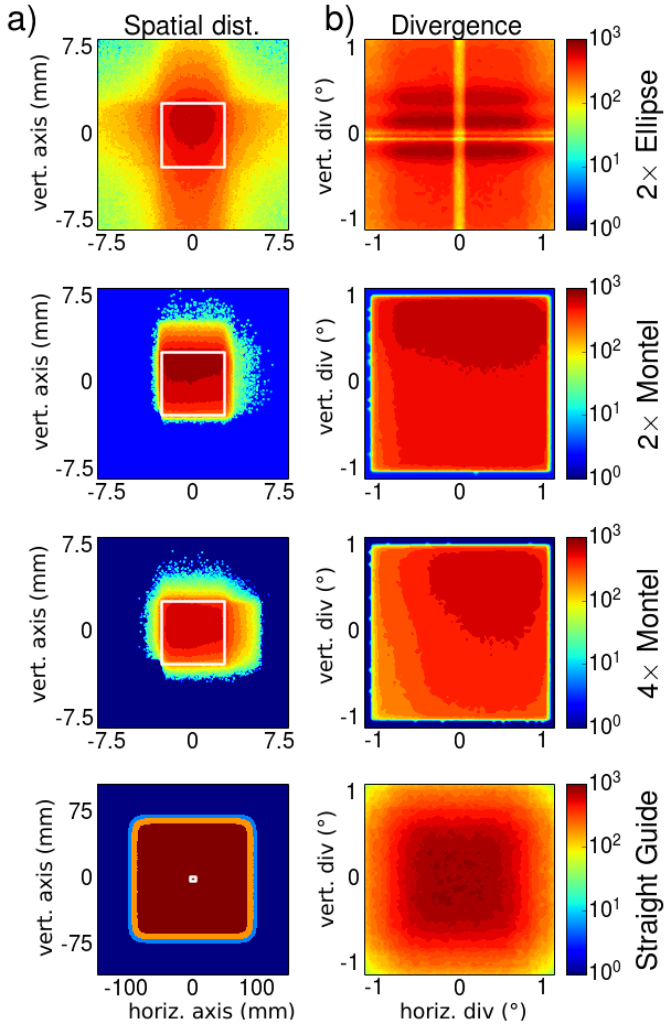

Figure 7: Spatial (a) and divergence (b) intensity distribution at the sample position for the different guide systems integrated over a flat wavelength spectrum of 2 Å – 6 Å. The left side (a) shows monitor images of the spatial distribution of the neutrons with gravity and the right side (b) the divergence distribution, respectively. The white rectangle in (a) marks the sample with a size of 5×5 mm^2, which corresponds to the opening aperture for the elliptic guide and the Montel guide system. The straight guide was simulated without aperture.

In a further study one may also consider more advanced geometries for Montel optics such as systems being composed of parabolic Montel mirrors at the entrance and the exit of a guide system connected via a long straight guide section. Such a geometry may reduce the effects of gravity further.

In the future, it may become possible to build neutron sources based on the ejection of photo neutrons from halo isomers by means of γ- and laser beams, which will provide neutron beams with a very high brilliance [21] and a small diameter of the order of 0.1 mm. The small beam size leads to short mirrors and therefore effects of gravity become a minor issue.

5. Acknowledgements

This work was funded by the German BMBF under “Mitwirkung der Zentren der Helmholtz Gemeinschaft und der Technischen Universität München an der Design-Update Phase der ESS, Förderkennzeichen 05E10WO1.”

References

[1] Yellow Book of the ILL, p 4–6, 2008.

[2] H. Maier-Leibnitz, T. Springer, The use of neutron optical devices on beam-hole experiments on beam-hole experiments, Journal of Nuclear Energy. Parts A/B. Reactor Science and Technology 17 (4–5) (1963) 217 – 225, ISSN 0368-3230, doi:http://dx.doi.org/10.1016/0368-3230(63)90022-3, URL http://www.sciencedirect.com/science/article/pii/036832306390022

[3] SwissNeutronics, Neutron Supermirrors, URL http://www.swissneutronics.ch/products/coatings.html, 2014.

[4] P. Böni, F. Grünauer, C. Schanzer, Shielding of elliptic guides with direct sight to the moderator, Nuclear Instruments and Methods in Physics Research Section A: Accelerators, Spectrometers, Detectors and Associated Equipment 624 (1) (2010) 162 – 167, ISSN 0168-9002, doi:http://dx.doi.org/10.1016/j.nima.2010.09.015, URL http://www.sciencedirect.com/science/article/pii/S01689002100197

[5] F. Mezei, J. Neutron Res. 6 (1997) 3.

[6] C. Schanzer, P. Böni, U. Filges, T. Hils, Advanced geometries for ballistic neutron guides, Nuclear Instruments and Methods in Physics Research Section A: Accelerators, Spectrometers, Detectors and Associated Equipment 529 (1–3) (2004) 63 – 68, ISSN 0168-9002, doi:http://dx.doi.org/10.1016/j.nima.2004.04.178, URL http://www.sciencedirect.com/science/article/pii/S01689002040086 proceedings of the Joint Meeting of the International Conference on Neutron Optics (NOP2004) and the Third International Workshop on Position-Sensitive Neutron Detectors (PSND2004).

[7] L. D. Cussen, D. Nekrassov, C. Zendler, K. Lieutenant, Multiple reflections in elliptic neutron guide tubes, Nuclear Instruments and Methods in Physics Research Section A: Accelerators, Spectrometers, Detectors and Associated Equipment 705 (0) (2013) 121 – 131.

[8] R. M. Ibberson, Design and performance of the new supermirror guide on HRPD at ISIS, Nuclear Instruments and Methods in Physics Research, Section A: Accelerators, Spectrometers, Detectors and Associated Equipment 600 (2009) 47–49, ISSN 01689002, doi: 10.1016/j.nima.2008.11.066.

[9] P. Böni, High Intensity Neutron Beams for Small Samples, Journal of Physics: Conference Series 502 (1) (2014) 012047, URL http://stacks.iop.org/1742-6596/502/i=1/a=012047.

[10] K. H. Klenø, K. Lieutenant, K. H. Andersen, K. Lefmann, Systematic performance study of common neutron guide geometries, Nuclear Instruments and Methods A 696 (2012) 75–84, URL http://gateway.webofknowledge.com/gateway/Gateway.cgi?GWVersion=papers2://publication/doi/10.1016/j.nima.2012.08.027.

[11] P. Böni, New concepts for neutron instrumentation, Nuclear Instruments and Methods in Physics Research, Section A: Accelerators, Spectrometers, Detectors and Associated Equipment 586 (2008) 1–8, ISSN 01689002, doi:10.1016/j.nima.2007.11.059.

[12] C. Zendler, D. Nekrassov, K. Lieutenant, An improved elliptic guide concept for a homogeneous neutron beam without direct line of sight, Nuclear Instruments and Methods in Physics Research Section A: Accelerators, Spectrometers, Detectors and Associated Equipment 746 (0) (2014) 39 – 46, ISSN 0168-9002, doi:http://dx.doi.org/10.1016/j.nima.2014.01.044, URL http://www.sciencedirect.com/science/article/pii/S0168900214000953.

[13] K. H. Klenø, P. K. Willendrup, E. Knudsen, K. Lefmann, Eliminating line of sight in elliptic guides using gravitational curving, Nuclear Instruments and Methods A 634 (1) (2011) 0, URL http://pubget.com/site/paper/pgtmp_1ba3576f617a94c74d2d1c252ff4f5df?institution=papers2://publication/doi/10.1016/j.nima.2010.06.261.

[14] M. Montel, X-ray microscopy with catamegonic roof mirrors, X-ray microscopy and microradiography, Academic Press, 1957.

[15] G. E. Ice, J. W. L. Pang, C. Tulk, J. Molaison, J.-Y. Choi, C. Vaughn, L. Lytle, P. Z. Takacs, K. H. Andersen, T. Bigault, A. Khounsary, Design challenges and performance of nested neutron mirrors for microfocusing on SNAP, Journal of Applied Crystallography 42 (6) (2009) 1004–1008, doi:10.1107/S0021889809037595, URL http://dx.doi.org/10.1107/S0021889809037595.

[16] J. Stahn, U. Filges, T. Panzner, Focusing specular neutron reflectometry for small samples, The European Physical Journal Applied Physics 58, ISSN 1286-0050, doi:10.1051/epjap/2012110295.

[17] T. Weber, G. Brandl, R. Georgii, W. Häußler, S. Weichselbaumer, P. Böni, Monte-Carlo simulations for the optimisation of a TOF-MIEZE instrument, Nuclear Instruments and Methods in Physics Research Section A: Accelerators, Spectrometers, Detectors and Associated Equipment 713 (0) (2013) 71 – 75, ISSN 0168-9002, doi:http://dx.doi.org/10.1016/j.nima.2013.03.010.

[18] J. Stahn, T. Panzner, U. Filges, C. Marcelot, P. Böni, Study on a focusing, low-background neutron delivery system, Nuclear Instruments and Methods in Physics Research Section A: Accelerators, Spectrometers, Detectors and Associated Equipment 634 (1, Supplement) (2011) S12 – S16, ISSN 0168-9002, doi:http://dx.doi.org/10.1016/j.nima.2010.06.221, URL http://www.sciencedirect.com/science/article/pii/S0168900210014117, proceedings of the International Workshop on Neutron Optics NOP2010.

[19] P. Willendrup, E. Knudsen, K. Lefmann, E. Farhi, U. Filges, McStas – A neutron ray-trace simulation package, URL http://mcstas.org, 2014.

[20] ESS, Scientific & Technological Documentation, URL http://europeanspallationsource.se/scientific-technological-documentation, 2013.

[21] D. Habs, M. Gross, P. Thirolf, P. Böni, Neutron halo isomers in stable nuclei and their possible application for the production of low energy, pulsed, polarized neutron beams of high intensity and high brilliance, Applied Physics B 103 (2) (2011) 485–499, ISSN 0946-2171, doi:10.1007/s00340-010-4276-3, URL http://dx.doi.org/10.1007/s00340-010-4276-3.